

# Oncolytic Immunotherapy for Bladder Cancer Using Coxsackie A21 Virus

Nicola E. Annels,<sup>1</sup> Mehreen Arif,<sup>1</sup> Guy R. Simpson,<sup>1</sup> Mick Denyer,<sup>1</sup> Carla Moller-Levet,<sup>1</sup> David Mansfield,<sup>2</sup> Rachel Butler,<sup>1</sup> Darren Shafren,<sup>3</sup> Gough Au,<sup>3</sup> Margaret Knowles,<sup>5</sup> Kevin Harrington,<sup>2</sup> Richard Vile,<sup>4</sup> Alan Melcher,<sup>2</sup> and Hardev Pandha<sup>1</sup>

<sup>1</sup>Department of Clinical and Experimental Medicine, Faculty of Health and Medical Science, Leggett Building, Daphne Jackson Road, University of Surrey, Guildford GU2 7WG, UK; <sup>2</sup>The Institute of Cancer Research, London SM2 5PT, UK; <sup>3</sup>Viralitics Limited, Suite 305, Level 3, 66 Hunter Street, Sydney, NSW 2000, Australia; <sup>4</sup>Department of Molecular Medicine, Mayo Clinic, Rochester, MN 55902, USA; <sup>5</sup>Section of Experimental Oncology, Leeds Institute of Cancer and Pathology, St. James's University Hospital, Beckett Street, Leeds LS9 7TF, UK

**As a clinical setting in which local live biological therapy is already well established, non-muscle invasive bladder cancer (NMIBC) presents intriguing opportunities for oncolytic virotherapy. Coxsackievirus A21 (CVA21) is a novel intercellular adhesion molecule-1 (ICAM-1)-targeted immunotherapeutic virus. This study investigated CVA21-induced cytotoxicity in a panel of human bladder cancer cell lines, revealing a range of sensitivities largely correlating with expression of the viral receptor ICAM-1. CVA21 in combination with low doses of mitomycin-C enhanced CVA21 viral replication and oncolysis by increasing surface expression levels of ICAM-1. This was further confirmed using 300- $\mu$ m precision slices of NMIBC where levels of virus protein expression and induction of apoptosis were enhanced with prior exposure to mitomycin-C. Given the importance of the immunogenicity of dying cancer cells for triggering tumor-specific responses and long-term therapeutic success, the ability of CVA21 to induce immunogenic cell death was investigated. CVA21 induced immunogenic apoptosis in bladder cancer cell lines, as evidenced by expression of the immunogenic cell death (ICD) determinant calreticulin, and HMGB-1 release and the ability to reject MB49 tumors in syngeneic mice after vaccination with MB49 cells undergoing CVA21 induced ICD. Such CVA21 immunotherapy could offer a potentially less toxic, more effective option for the treatment of bladder cancer.**

## INTRODUCTION

Urothelial cancer of the bladder is the seventh most common cancer in the UK, with over 10,000 new cases annually in the UK.<sup>1</sup> Superficial, non-muscle invasive bladder cancers (NMIBCs) are managed with cystoscopic transurethral resection of all visible lesions followed by intravesical chemotherapy and/or immunotherapy.<sup>2</sup> The use of Bacillus Calmette-Guerin (BCG) as an immunotherapy for NMIBC and its proven effects of reducing recurrence and progression and improving disease-specific survival revolutionized the treatment of this malignancy in the 1970s. However, the potential for serious side effects of local and systemic BCG infection as well as the fact that there is a significant (30%) group of non-responder patients to BCG highlights the

need to develop future immune-based therapies that overcome these problems.<sup>3</sup> The precise mechanisms underpinning the clinical efficacy of BCG remain unclear. Urothelial cells (including bladder cancer cells themselves) and various components of the immune system both have crucial roles. The possible involvement of bladder cancer cells includes attachment and internalization of BCG, secretion of cytokines and chemokines, and presentation of BCG and/or cancer cell antigens to cells of the immune system. Immune cell subsets that have potential roles in BCG therapy include CD4<sup>+</sup> and CD8<sup>+</sup> lymphocytes, natural killer cells, granulocytes, macrophages, and dendritic cells. Bladder cancer cells are killed through direct cytotoxicity by these cells; by secretion of soluble factors, such as TRAIL (tumor-necrosis-factor-related apoptosis-inducing ligand); and, to some degree, by the direct action of BCG. New agents are vital, capable of the immunotherapeutic effects of BCG but without the toxicity and need to use a potentially hazardous live agent in the clinic. The accessibility and superficial location of NMIBC allows direct intravesical administration of antitumor agents and is an ideal model for evaluation of new therapies as, through insertion of a conventional urinary catheter, precise modulation of infusion volume, infusion rate, time of retention in the bladder by catheter clamping, as well as frequency of treatments can be precisely undertaken as well as combination with other agents. Alternatives to BCG have been long sought, due to its toxicity and limited efficacy and, also in recent years, the difficulty with its manufacture.<sup>4,5</sup> Viruses, both non-replication for gene transfer and replication-competent oncolytic viruses (OVs), have been evaluated for the treatment of NMIBC. These viruses infect and selectively lyse tumor cells, leaving non-transformed cells unharmed.<sup>6,7</sup>

The roles of the host immune system in contributing to the therapeutic activity of OV through intratumoral and systemic delivery are now

Received 5 February 2018; accepted 6 February 2018;  
<https://doi.org/10.1016/j.omto.2018.02.001>.

**Correspondence:** Hardev Pandha, Department of Clinical and Experimental Medicine, Faculty of Health and Medical Science, Leggett Building, Daphne Jackson Road, University of Surrey, Guildford GU2 7WG, UK.

**E-mail:** [h.pandha@surrey.ac.uk](mailto:h.pandha@surrey.ac.uk)



well recognized.<sup>8–10</sup> Emerging evidence has shown that oncolytic virotherapy induces immunogenic cell death (ICD).<sup>11–13</sup> This is characterized by expression of potent danger signals, such as alterations in the composition of the plasma membrane of dying cells (including surface-exposed calreticulin [ecto-CRT] and heat shock proteins), as well as release of ATP and high-mobility group box 1 protein (HMGB-1). These are thought to be the optimal way to trigger activation of the immune system against cancer, ultimately resulting in long-term success of virotherapy.<sup>14</sup> Coxsackievirus A21 (CVA21), a naturally occurring “common cold” intercellular adhesion molecule-1 (ICAM-1)-targeted RNA virus, has exhibited selective oncolytic activity in a range of solid tumors.<sup>15–19</sup> CAVATAK is a novel bio-selected formulation of CVA21, whose oncolytic and immunotherapeutic capacity has already been clearly demonstrated in *in vitro* cultures, *in vivo* melanoma models, and several human trials where CAVATAK has been administered intratumorally alone or in combination with immune checkpoint inhibitors, resulting in significant bystander effects with reduction of distant non-injected metastases.<sup>20</sup>

We evaluated CVA21 as a novel oncolytic virus for the treatment of human bladder cancer. Bladder cancer cell lines were assessed for surface expression of the viral receptors ICAM-1 and decay accelerating factor (DAF) by flow cytometry and subsequent susceptibility to viral-induced lytic infection. We hypothesized that lytic infection could be facilitated/enhanced by treatment of bladder cancer cell lines with Mitomycin-C by increasing ICAM-1 expression on the surface of the bladder cancer cells. Furthermore, we investigated the mode of cell death induced by CVA21 and potential immunogenicity in an immunocompetent murine bladder cancer model.

## RESULTS

### Susceptibility of Bladder Cancer Cell Lines to CVA21 Infection

Monolayers of each of the ten bladder cancer cell lines were inoculated with CVA21 at MOIs from 0 to 50 and cell viability quantified 72 hr post-infection using the 3-(4,5-dimethylthiazol-2-yl)-2,5-diphenyltetrazolium bromide (MTS) colorimetric cell-viability assay. As shown in Figure 1A, cell viability was significantly decreased in the 253J, VM-UB2, HCV29, T24, TCCSUP, and 5637 cell lines compared to J82, KU19-19, VMCUB1, and RT-112 at MOIs  $\geq 1.0$ . Heat-inactivated CVA21 did not affect the cell viability over the range of MOIs tested, demonstrating that live CVA21 was required for oncolytic potency (Figure S1A).

To confirm whether or not CVA21 was entering the least susceptible bladder cancer cell lines, the distribution of CVA21 was examined 24 hr post-infection in the bladder cancer cell lines using immunofluorescence and confocal microscopy. The six most susceptible bladder cancer cell lines, 253J, VM-CUB2, HCV29, T24, 5637, and TCCSUP, all showed CVA21 distributed in the cytoplasm, often with a peri-nuclear localization. Despite the apparent lack of susceptibility to the virus, J82 and KU19-19 cell lines also demonstrated clear infectivity by CVA21 in contrast to VMCUB and RT-112 that remained refractile to infection (Figure 1A).

### Expression of ICAM-1 and DAF on Bladder Cancer Cell Lines

To determine whether the infectivity of the bladder cancer cell lines was due to their viral receptor expression profiles, the surface expression of ICAM-1 and DAF was examined by flow cytometric analysis. Whereas all cancer cell lines expressed a high level of DAF, only the most susceptible cell lines, 253J, VM-CUB2, HCV29, T24, TCCSUP, and 5637, also expressed a high level of ICAM-1, with the exception of J82, which despite expressing ICAM-1 to similar levels still did not succumb to viral infection (Figure 1B). Of note, J82 was the only cell line that showed a significant increase in the antiviral cytokine, interferon (IFN)  $\beta$ , post-CVA21 treatment (Figure S2). A lower level of ICAM-1 was observed on the KU19-19 and VMCUB1 cell lines and minimal to no surface ICAM-1 on the RT-112 cells (Figure 1B). Quantification of the mean absolute number of membrane-bound ICAM-1 molecules per cell using QuantiBRITE PE calibration beads further confirmed this differing viral receptor expression profile for the bladder cancer cell lines (Figure 1C). These results indicated that a threshold of at least 5,000 ICAM-1 molecules per cell was required in order for the virus to exhibit activity.

To further demonstrate the importance of ICAM-1 expression for viral infectivity, the KU19-19 cell line that had been shown to display a small subset of ICAM-1-positive cells was sorted into ICAM-1-positive and negative subsets and the susceptibility of these sorted populations to virus assessed as before 72 hr post-infection using the MTS colorimetric cell-viability assay. As shown in Figure 1D, the ICAM-1-negative population showed no susceptibility to the virus, whereas the ICAM-1-positive cells showed enhanced susceptibility compared to the negative population and whole unsorted KU19-19 cells.

It has been reported that oncogenic Kras mutations in pancreatic acinar cells induce the expression of ICAM-1.<sup>21</sup> However, in the bladder cancer cell lines we studied, the Sanger COSMIC database<sup>22</sup> showed no common genomic mutations in one or more of a set of genes (PIK3CA, RB1, RAS, TSC1, CDKN2A, PTEN, and TP53) associated with ICAM-1 expression or the susceptibility of particular bladder cancer cell lines to CVA21 infection.

### *In Vitro* Survival of Cells following Treatment with a Combination of CVA21 and Chemotherapy

Unpublished work from our group had shown that radiation upregulates expression of the ICAM-1 cell surface receptor on bladder cancer cell lines. However, as radiation is not normally used as a treatment for NMIBC, the commonly used chemotherapy, Mitomycin C, was tested on six bladder cancer cell lines to determine any effects on ICAM-1 receptor expression. Bladder cancer cell lines T24, TCCSUP, and 5637 were treated with increasing doses of Mitomycin-C (0.05–4  $\mu\text{g}/\text{mL}$ ) for an hour and the mean fluorescence intensity of ICAM-1 expression determined by flow cytometry after incubation in growth media for 24, 48, and 72 hr. Cytotoxic effects of Mitomycin-C were assessed using the live/dead cell discriminator, ViViD. Figure 2A shows that, at low doses of Mitomycin-C (up to 0.5  $\mu\text{g}/\text{mL}$ ), ICAM-1 surface expression increased in all three cell lines without any significant cytotoxic effects. This increase in Mitomycin-C-induced ICAM-1 expression was further confirmed at the RNA level in the 5637 cell line. RNA was

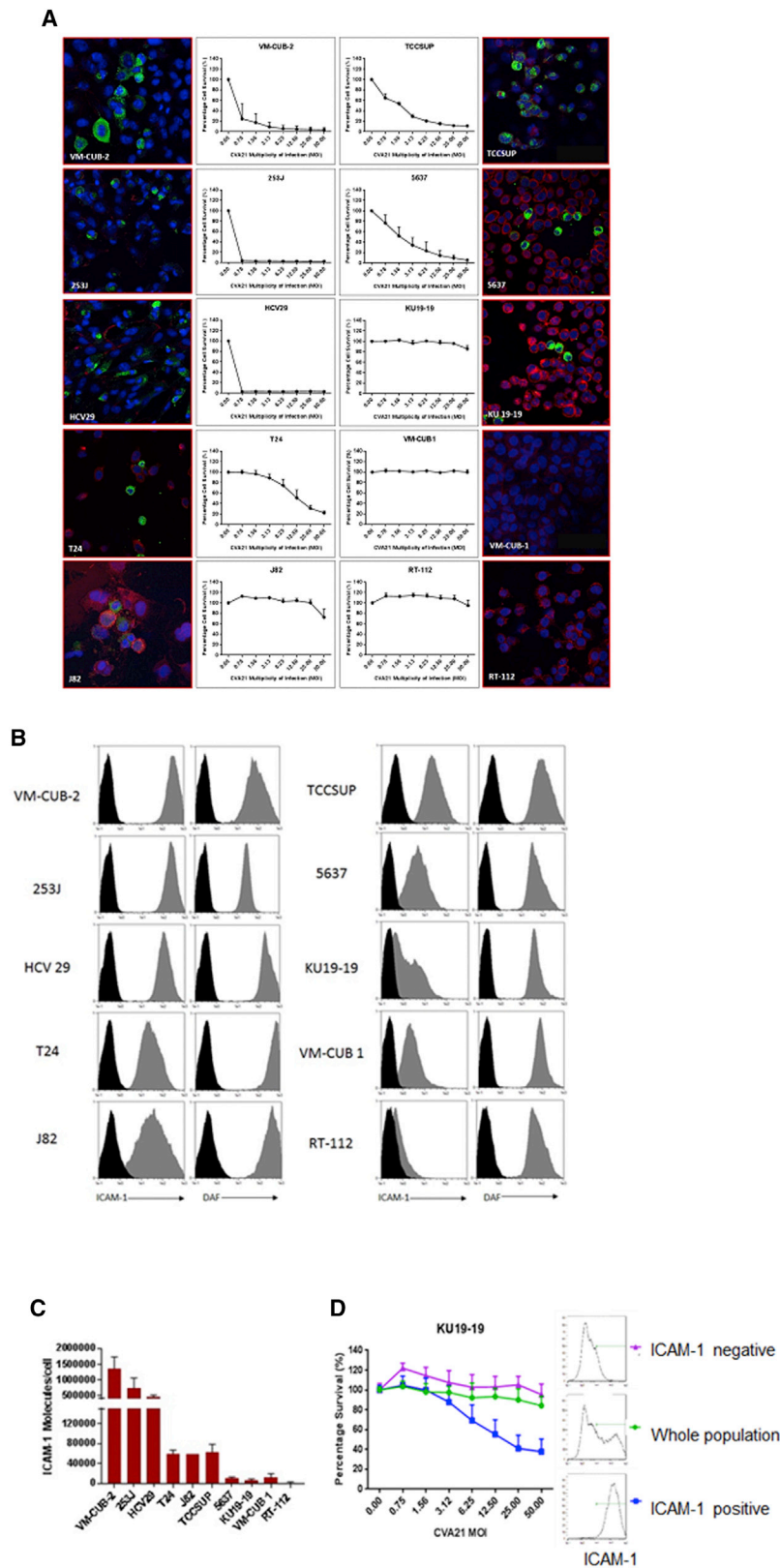


**Figure 1. Susceptibility of Bladder Cancer Cell Lines to CVA21 Infection and Expression Profile of Surface ICAM-1 and DAF on Bladder Cancer Cell Lines**

(A) Monolayer cultures of human bladder cancer cells were challenged with increasing multiplicities of CVA21 and assessed for cell survival at 72 hr post-infection, with live cells being quantified by MTS assay. Confocal images of human bladder cancer cell lines 24 hr post-CVA21 infection are shown (green, CVA21 viral proteins; red, wheat germ agglutinin; blue, nuclei stained with TO-PRO-3). Magnification 40 $\times$  is shown. (B) Surface expression of ICAM-1 and DAF on bladder cancer cell lines was determined by flow cytometry. Cell lines were incubated with the relevant PE-conjugated isotype control antibody (black histogram), anti-DAF monoclonal antibody, or anti-ICAM-1 monoclonal antibody (gray histogram). (C) Absolute numbers of ICAM-1 molecules on bladder cancer cells were determined by QuantiBRITE PE analysis. (D) KU19-19 bladder cancer cells were stained with an anti-ICAM-1-PE antibody and sorted into ICAM-1-positive or negative populations using magnetic enrichment of PE-positive cells. Together with the whole unsorted KU19-19 population, the different fractions were challenged with increasing multiplicities of CVA21 and assessed for cell survival at 72 hr post-infection, with live cells being quantified by MTS assay.

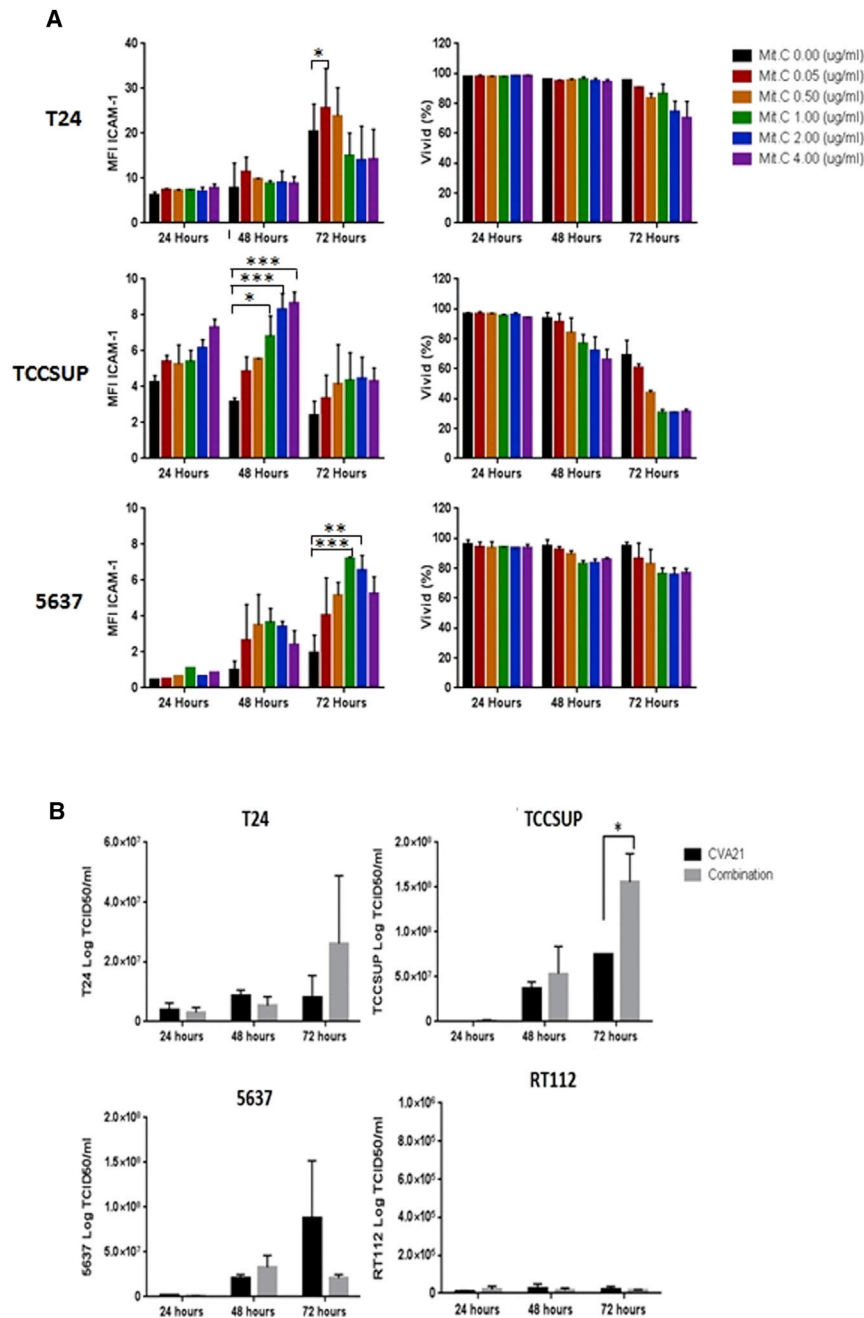


**Figure 2. The Effects of Mitomycin-C on Bladder Cancer Cells and Viral Replication**

(A) Low doses of Mitomycin-C upregulate ICAM-1 protein expression with minimal cytotoxic effects. Bladder cancer cell lines were either left untreated or treated with Mitomycin-C at increasing doses for one hour before determining the mean fluorescence intensity (MFI) of ICAM-1 expression by flow cytometry after 24, 48, and 72 hr. The cells were also assessed for any cytotoxicity using the live/dead cell discriminator, ViVid. Data represent averaged results from two independent experiments, and two-way ANOVA statistical analysis was performed. \* $p < 0.05$ ; \*\* $p < 0.01$ ; \*\*\* $p < 0.001$ ; \*\*\*\* $p < 0.0001$ . (B) Effect of Mitomycin-C on CVA21 replication in bladder cancer cell lines is shown. Bladder cancer cell lines were treated with or without 0.5  $\mu\text{g/mL}$  Mitomycin-C for 1 hr before infecting with CVA21 at MOI of 11.44 for T24, 1.0 for TCCSUP, 1.8 for 5637, and 25 for RT112. Supernatants were harvested 24, 48, and 72 hr after infection, and viral titers were measured by standard plaque assays on SKMEL-28 cell monolayers. Graphs represent pooled data from two independent experiments. \* $p < 0.05$ .

itates CVA21 entry and thus enhanced viral replication, viral titers were measured by standard plaque assays on SKMEL-28 cell monolayers. Three susceptible bladder cancer cell lines (T24, TCCSUP, and 5637) and as a control one refractile cell line (RT-112) were treated with or without 0.5  $\mu\text{g/mL}$  Mitomycin-C for 1 hr before infecting with CVA21 for 5 hr and incubation in growth media for 24, 48, and 72 hr post-infection. Cell supernatant was collected for extracellular virus quantification. The results showed that, in the T24 and TCCSUP cells, there were increased virus yields by 72 hr in the combination-treated cells compared to virus alone. This was true for the 5637 cell line up to 48 hr but then virus yield fell by 72 hr, probably due to significant cell death in this culture. RT-112, which had been shown to be refractile to infection, showed no change in virus yield with either treatment condition (Figure 2B). Similarly, Mitomycin-C treatment of the ICAM-1-negative sorted cells from the cell line KU19-19 also did not induce ICAM-1 expression on these cells, and they re-

extracted from the 5637 cell line, which had been treated with doses of Mitomycin-C up to 0.8  $\mu\text{g/mL}$ , and qPCR performed. Figure S3 shows upregulated expression of ICAM-1 along with another viral receptor DAF in the 5637 cell line in response to increasing doses of Mitomycin-C treatment.

To investigate whether the increased ICAM-1 viral receptor expression induced by Mitomycin-C treatment of bladder cancer cells facil-

it remained insensitive to the virus (data not shown). These results suggest that, in ICAM-1-expressing bladder cancer cells, Mitomycin-C treatment can increase further the ICAM-1 surface expression, thus facilitating enhanced CVA21 uptake and subsequent replication.

#### Induction of Death by CVA21 in Bladder Cancer Cells

To characterize the cell death pathways involved, the presence of apoptosis markers after treatment with Mitomycin-C, CVA21, or

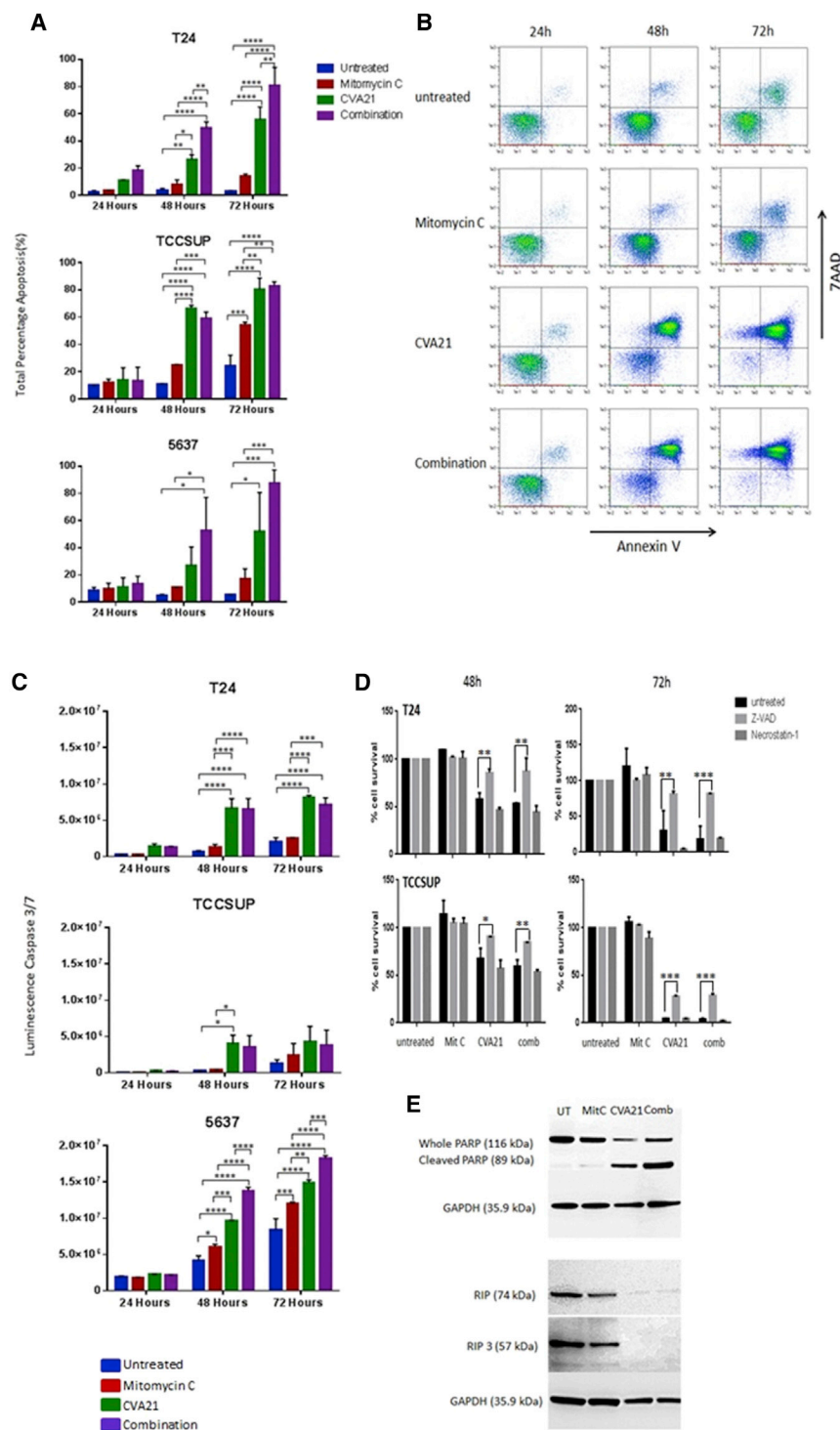


**Figure 3. CVA21-Induced Cell Death of Bladder Cancer Cell Lines**

(A) Determination of levels of apoptosis in three bladder cancer cell lines left untreated or treated with Mitomycin-C, CVA21, or the combination at 24, 48, and 72 hr post-treatment by means of annexin-V- and 7AAD-based flow cytometry. Graphs represent pooled data from two independent experiments, and the statistical significance of the treatment group comparisons was analyzed using two-way ANOVA; \* $p < 0.05$ ; \*\* $p < 0.01$ ; \*\*\* $p < 0.001$ ; \*\*\*\* $p < 0.0001$ . (B) Representative dot plots recorded for TCCSUP cells following the different treatments at 24, 48, and 72 hr post-treatment are shown. (C) Apoptosis (quantified via caspase 3/7 activity) in three bladder cancer cell lines left untreated or treated with Mitomycin-C, CVA21, or the combination at 48 and 72 hr post-treatment is shown. Graphs represent pooled data from two independent experiments, and the statistical significance of the treatment group comparisons was analyzed using two-way ANOVA; \* $p < 0.05$ ; \*\* $p < 0.01$ ; \*\*\* $p < 0.001$ ; \*\*\*\* $p < 0.0001$ . (D) Increase in percentage cell survival was seen in CVA21 and combination-treated cells with Z-VAD-FMK, apoptosis inhibitor, whereas the necroptosis inhibitor, necrostatin-1, failed to increase cell survival in bladder cancer cell lines treated with CVA21 alone or in combination with Mitomycin-C. Graphs represent pooled data from two independent experiments, and the statistical significance of the treatment group comparisons was analyzed using two-way ANOVA; \* $p < 0.05$ ; \*\* $p < 0.01$ ; \*\*\* $p < 0.001$ ; \*\*\*\* $p < 0.0001$ . (E) Western blot analysis demonstrating absence of RIP1 and RIP3 necroptosis markers but upregulation of cleaved PARP in TCCSUP cells 72 hr post-CVA21 infection is shown.

the combination were assessed. Annexin V-7AAD-based fluorescence-activated cell sorting (FACS) analyses showed significant upregulation of annexin V staining at 48 hr and 72 hr after CVA21 infection in all three bladder cancer cell lines tested. This induction of cell

death was enhanced when cells had been pre-treated with Mitomycin-C (0.5  $\mu\text{g}/\text{mL}$ ). In contrast, Mitomycin-C treatment alone showed no significant cytotoxicity over the untreated control cells (Figures 3A and 3B). Further confirmation of this apoptotic cell death pathway induced by CVA21 was demonstrated by the activation of the effector caspases, caspase-3 and -7, 48 hr after infection (Figure 3C). Furthermore, pre-treatment with the pan-caspase chemical inhibitor zVAD rescued the cells from virus-induced death whereas necrostatin-1 had no effect (Figure 3D). To exclude the involvement of additional interconnected death pathways, western blotting of whole-cell lysates, untreated, Mitomycin-C treated, or CVA21 treated with or without Mitomycin-C, were analyzed using a PARP antibody (apoptosis marker) as well as RIP1 and RIP3 antibodies (necroptosis). The protein levels of RIP1 and RIP3 either decreased or did not change in any of the bladder cancer cell lines exposed to CVA21 and combination treatment whereas, in contrast, the whole PARP was cleaved, yielding

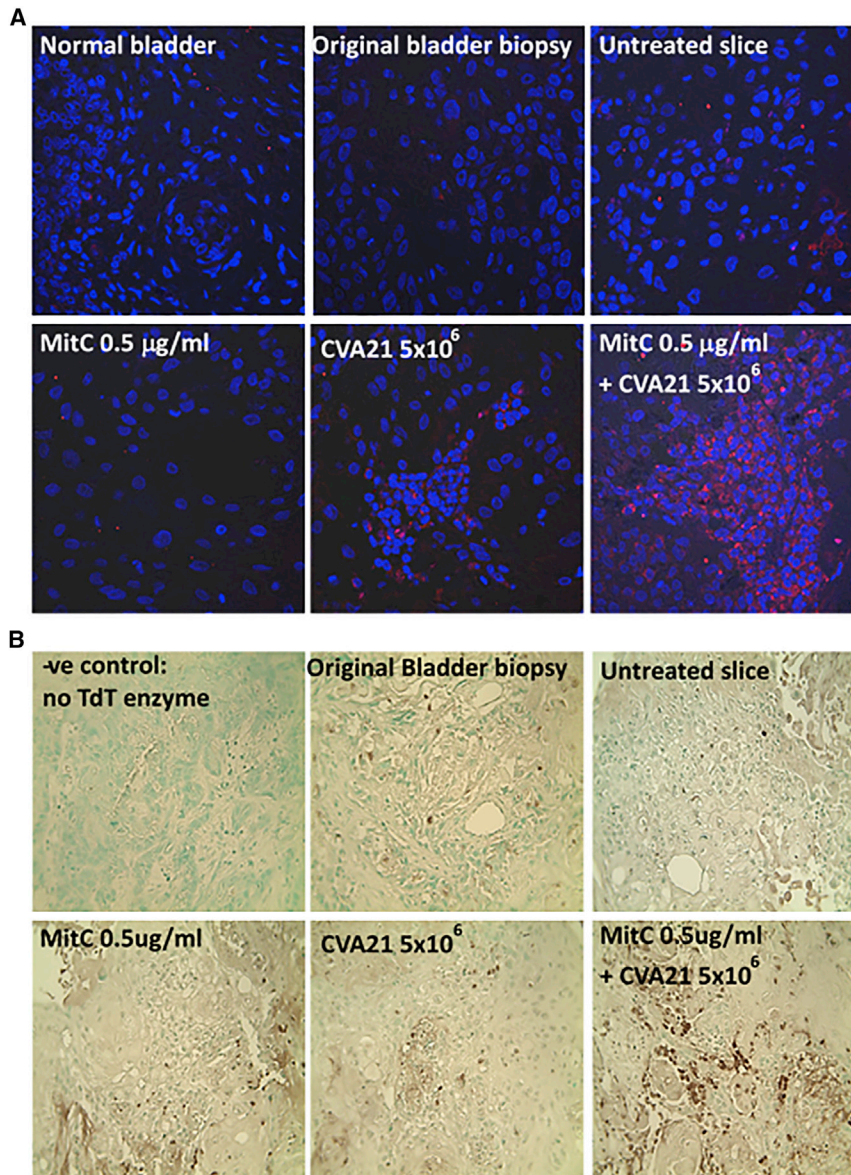


**Figure 4. Enhanced Cytotoxicity of Mitomycin-C and CVA21 on Bladder Cancer Tumor Slices**

Precision-cut slicing of resection material from a patient with squamous bladder cancer was performed using a vibratome. The 300- $\mu\text{m}$  slices were either left untreated or treated with Mitomycin-C, CVA21, or the combination and then cultured for 48 hr. Slices were then fixed, paraffin embedded, and 4- $\mu\text{m}$  sections prepared. These sections together with a section from the original biopsy were stained for (A) presence of viral protein (red) and the nuclear stain TO-PRO-3 (blue) and (B) evidence of apoptosis using the TumorTACS *in situ* apoptosis detection kit (apoptotic cells are identified by the dark brown staining). Magnification 40 $\times$  is shown.

which had not been exposed to any treatment but cultured for the same period, were fixed simultaneously and embedded in paraffin for histological analysis. Immunofluorescent staining for the presence of viral protein showed increased viral replication within the combination-treated slices as compared to the CVA21-alone-treated tumor slice (Figure 4A). As expected, there was no evidence of virus within the Mitomycin-C-treated or untreated slices. Furthermore, a significantly higher level of apoptotic activity within the combination-treated tissue slice as compared to CVA21- or Mitomycin-C-alone-treated slices was observed. The control slice had little to no evidence of apoptotic cells, reflecting the situation in the original tumor biopsy (Figure 4B).

#### Immunogenicity of Cell Death Induced by CVA21

In order to determine the immunogenic profile of CVA21-infected bladder cancer cell lines, 3 susceptible cell lines (T24, 5637, and TCCSUP) were infected with CVA21 at an MOI of 11.44 for T24, 1.0 for TCCSUP, and 1.8 for 5637 and

analyzed for expression of the ICD determinants calreticulin, HSP70, extracellular ATP, and high-mobility group box 1 (HMGB1) at 24, 48, and 72 hr. This treatment induced surface expression of ecto-calreticulin on two out of the three cell lines (T24 and 5637), which was particularly marked by 72 hr in the combination-treated cells (Figure 5A). No significant changes in surface expression of HSP70 were observed in any of the cell lines studied (data not shown). The secreted danger signal, HMGB1, was evident in the culture medium of CVA21 and combination-treated bladder cancer cells at 48 and 72 hr post-treatment (Figure 5B); however, no specific upregulation of extracellular ATP in response to CVA21 infection could be detected. Of note, infection with heat-inactivated virus did not induce upregulation of the ICD markers calreticulin or HMGB1, indicating the need for a productive CVA21 infection to facilitate immunogenic cell death (Figure S1B).

#### Enhanced Cytotoxicity of Mitomycin-C and CVA21 on Bladder Cancer Slices

To test the combination treatment of CVA21 and Mitomycin-C in a preclinical model system that represents both tumor architecture, heterogeneity, and the complexity of a tumor *in situ*, we took advantage of a fresh bladder tumor specimen that came into our lab from which 300- $\mu\text{m}$  precision-cut slices of tumor were prepared. Slices with or without pre-treatment with Mitomycin-C (0.5  $\mu\text{g}/\text{mL}$ ) for 1 hr were infected with CVA21 ( $5 \times 10^6$  plaque-forming units [PFU]/mL) and cultured for 48 hr. Control slices of the same tumor,

an 89-kD PARP fragment (Figure 3E). Altogether, these data indicated that the main mechanism for CVA21-induced cell death in bladder cancer cells was induction of apoptosis.

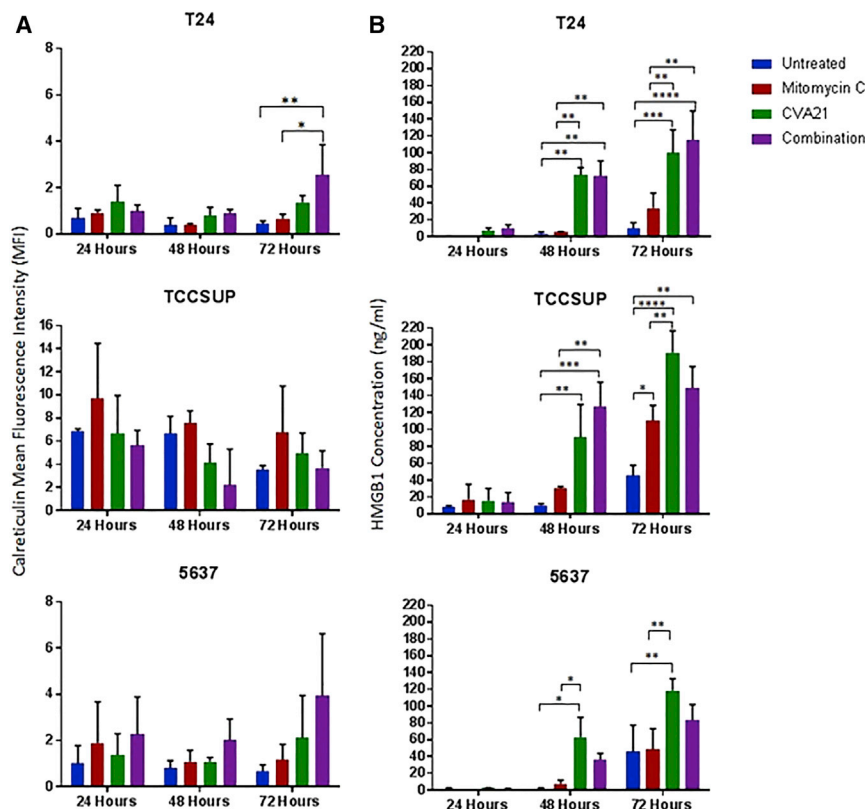


**Figure 5. Selective Induction of HMGB1 and Calreticulin by CVA21 Infection of Bladder Cancer Cells**

The bladder cancer cell lines, T24, TCCSUP, and 5637, were either left untreated or treated with Mitomycin-C (0.5  $\mu\text{g}/\text{mL}$ ), CVA21, or the combination. Cells and supernatants were harvested at 24, 48, and 72 hr time points. Cell surface calreticulin (CRT) exposure was determined by FACS analysis of the cells (A) whereas HMGB1 accumulation was determined by ELISA analysis of supernatants (B). Graphs represent pooled data from two independent experiments, and the statistical significance of the treatment group comparisons was analyzed using two-way ANOVA; \* $p < 0.05$ ; \*\* $p < 0.01$ ; \*\*\* $p < 0.001$ ; \*\*\*\* $p < 0.0001$ .

As the gold standard approach to evaluate the ability of a specific stimulus to cause bona fide ICD relies on vaccination assays,<sup>23</sup> a murine cancer model was developed using the mouse urothelial carcinoma cell line MB49 transfected with human ICAM-1 (Figure S4A). The susceptibility of the MB49/ICAM-1 cell line to CVA21 was shown by a significant decrease in cell viability compared to the wild-type MB49 cell line that remained refractile to infection (Figure S4B). Similar to the human bladder cancer cell lines, MB49/ICAM-1 cells exposed to the virus released the ICD determinant HMGB1 (Figure S4C). Thus, C57BL/6 mice were inoculated subcutaneously into the flank with lysates generated from MB49/ICAM-1 cells treated with or without CVA21 (Figure 6A). One week later, viable MB49 cells were introduced into the opposite flank and mice were monitored for the appearance of palpable neoplastic tumors. By day 18, 11 days after re-challenge, 100% of the mice that had initially received lysates from CVA21-treated MB49/ICAM-1 cells had been effectively vaccinated compared to 50% of the mice that had initially received untreated MB49/ICAM-1 cell lysates. As expected, the control mice all developed rapidly growing subcutaneous tumors.

In order to evaluate which immune cell population(s) were functionally important in the protection of the vaccinated mice against re-challenge with MB49 tumor cells, depletion was conducted one day prior to initial vaccination using anti-CD8, anti-CD4, or anti-NK monoclonal antibodies (mAbs). Only the mice depleted of CD4 cells

showed a rapid outgrowth of tumors upon re-challenge with live MB49 wild-type (WT) cells, with 82% of the animals succumbing to disease by the end of the study period. Mice depleted of CD8<sup>+</sup> T cells and natural killer (NK) cells showed comparable antitumor protection to immunoglobulin (Ig) control-treated mice, indicating that these cells do not play an important role in the therapeutic effect (Figure 6B). As expected, the control mice that had been vaccinated with only the MB49 cell lysate showed significant tumor outgrowth compared to the isotype control, CD8<sup>-</sup>, and NK-depleted groups. Collectively, these data showed for the first time an important role for CD4 cells in the therapeutic response mediated by vaccination with CVA21 MB49/ICAM-1 lysates.

## DISCUSSION

Treatment options and their outcomes in NMIBC have not changed significantly in decades. Whereas BCG continues to be the standard of care in patients with high-grade superficial disease, this is at a significant cost in terms of morbidity associated with BCG, the frequency and duration of treatments, and propensity to recur. NMIBC has been the focus of previous studies using an intravesical route of administration for a number of non-replicating viruses and OV's and reviewed recently.<sup>24</sup> We have previously shown, using an *in vivo* orthotopic bladder tumor model, that the use of an oncolytic herpes-simplex virus-1 (Oncovex(GALV/CD)) resulted in enhanced local tumor control by combining oncolysis with the expression of a highly potent pro-drug activating gene and the fusogenic glycoprotein.<sup>25</sup> Other viruses have been evaluated, including reovirus<sup>26</sup> and vaccinia.<sup>27</sup> The most advanced studies in humans involve CG0070, a selectively replicating adenovirus expressing granulocyte macrophage colony-stimulating factor (GM-CSF), in which the human E2F-1 promoter drives expression of the E1A viral gene. CG0070 preferentially replicates in Rb protein-defective bladder cancer cells, resulting in production of GM-CSF that activates the host immune response.<sup>28</sup> The initial study focused on CIS, Ta, and T1 patients

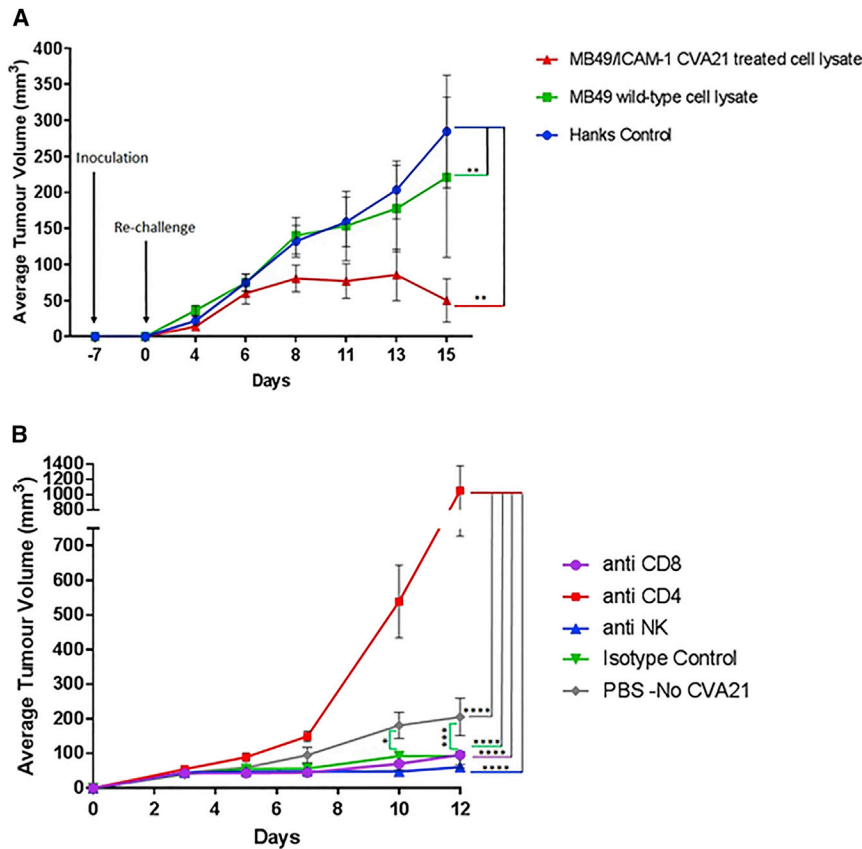


**Figure 6. CVA21-Induced ICD Effectively Vaccinates Mice**

(A) MB49 cells transfected with human ICAM-1 were treated with or without CVA21 for 24 hr, washed, and lysates prepared. These lysates along with HANKS media as a control were injected subcutaneously into one flank of immunocompetent syngeneic C57BL/6 mice (8 per group). One week later, mice were re-challenged with living MB49 cells, which were inoculated subcutaneously (s.c.) into the contralateral flank. Tumor incidence and growth were routinely monitored. Graphs represent pooled data from two independent experiments, and the means  $\pm$  SDs of 8 mice per group are shown. Two-way ANOVA statistical analysis was performed. \* $p < 0.05$ ; \*\* $p < 0.01$ ; \*\*\* $p < 0.001$ ; \*\*\*\* $p < 0.0001$ . (B) Depletion of CD8+, CD4+, and NK cells in C57BL/6 mice vaccinated with MB49/ICAM-1 lysates is shown. Depletions were conducted by intraperitoneal injections of purified mAbs 1 day before re-challenge with viable MB49 cells as well as throughout the duration of the experiment. Control mice had been vaccinated with wild-type MB49 cell lysate before re-challenge with viable MB49 cells and received no immune-cell-depleting antibodies. Tumor incidence and growth were monitored, and the statistical significance of the intergroup comparisons of tumor volumes was analyzed using two-way ANOVA. \* $p < 0.05$ ; \*\* $p < 0.01$ ; \*\*\* $p < 0.001$ ; \*\*\*\* $p < 0.0001$ .

with recurrent NMIBC cancer after BCG treatment and led to the current ongoing phase 3 trial for high-grade NMIBC patients who failed BCG therapy and refused cystectomy.<sup>29</sup>

Following the success of immune checkpoint inhibition in advanced bladder cancer, there are numerous trials evaluating the role of anti-PD-1 agents in NMIBC. Given the limited effect in advanced disease (25% response rate; median duration 12 months; recently reviewed)<sup>30</sup> and the potential toxicities of this form of immunotherapy in an older population, there is still an urgent need for improved, less toxic local agents for long-term tumor control. This study demonstrates the potential of CVA21 as a new oncolytic immunotherapy agent whose anti-cancer activity can now be extended as a novel treatment approach to NMIBC. Whereas the majority of bladder cancer cell lines studied were susceptible to direct oncolysis by CVA21, we hypothesized that increasing the expression of the viral receptor, ICAM-1, would further enhance this oncolysis. Treatment of bladder cancer cell lines with Mitomycin-C, a commonly used chemotherapeutic agent for bladder cancer, upregulated surface expression of ICAM-1, resulting in increased viral replication and oncolysis. This was further demonstrated using precision-cut slices (organotypic cultures) from a squamous bladder carcinoma case. Culture of these slices with Mitomycin-C, CVA21, or the combination showed an increase in viral infectivity in the combination-treated slices, and this

also correlated with an increase in apoptosis within these slices compared to the virus or Mitomycin-C-treated alone slices. This facilitation of virus infection is important in the *in vivo* setting to ensure a sufficient amount and concentration of virus such that a robust oncolytic effect is initiated.

The direct cytotoxic effect of oncolytic viruses is important, but it is now well recognized that the anticancer effects of oncolytic viruses also come from the activation of innate and adaptive tumor-specific immunity<sup>31–34</sup> and the immunogenicity of dying or dead cancer cells.<sup>11,14</sup> Understanding the mode of cancer cell death induced by particular oncolytic viruses is important when considering these agents for cancer therapy. This study revealed that apoptosis was the primary death pathway induced by CVA21 in bladder cancer cell lines, as evidenced by annexinV-7AAD staining, activation of the effector caspases, caspase-3 and -7, and induction of cleaved PARP. To determine whether this CVA21-induced cell death was in fact immunogenic, the *in vitro* characteristics of ICD in bladder cancer cell lines were investigated. Three damage-associated molecular patterns (DAMPs) have been attributed a crucial role in the immunogenic potential of nearly all ICD inducers, the surface-exposed “eat me” signal calreticulin, the “find me” signal ATP, and passively released HMGB1<sup>11,22</sup> CVA21 infection, induced ecto-calreticulin and release of HMGB1; however, no specific secreted ATP could be detected. The importance of HMGB1 release for initiating an anti-tumor response in bladder cancer has previously been demonstrated



in the context of BCG. *In vivo* animal models have shown that tumor cells engineered to have decreased HMGB1 release fail to respond to intravesical BCG, thus demonstrating the requirement of HMGB1 release by urothelial carcinoma cells for an *in vivo* antitumor effect.<sup>35</sup> It is thought that HMGB1 signals through its principal receptor, RAGE, to alter the biology of bladder cancer cells as well as functioning to direct a host cellular immune response to the site of its release.<sup>36</sup>

In addition to the molecular DAMP signature, vaccination studies performed in this study showed the ability to reject MB49 tumors in syngeneic mice after vaccination with lysates from MB49/ICAM-1 cells undergoing CVA21-induced ICD. We found this was dependent on the activation of CD4<sup>+</sup>T cells and not on CD8<sup>+</sup>T cells or NK cells. This is in contrast to previous studies on reovirus, a double-stranded RNA virus whose antitumor efficacy depends upon activation of dendritic cells to stimulate both NK-cell- and CD8<sup>+</sup>T-cell-mediated cytotoxicity.<sup>34,37</sup> Although the role of CD4<sup>+</sup>Th cells in contributing helper functions that modulate activity of both antigen-presenting cells and cytotoxic CD8<sup>+</sup>T cells is well established,<sup>38</sup> there is growing evidence for CD4<sup>+</sup>Th cells having more direct antitumor effects.<sup>39–41</sup> Future studies are needed to precisely define the role of CD4<sup>+</sup>Th cells in response to CVA21-treated MB49/ICAM-1 vaccination.

This *in vivo* tumor-rejecting capacity induced by dying cancer cells in the absence of any adjuvant is considered as a prerequisite for an agent to be termed an ICD inducer.<sup>22</sup> Thus, CVA21 can now be added to the growing list of oncolytic virus strains that have been shown to induce the molecular requirements of ICD, namely coxsackie B3,<sup>42</sup> oncolytic adenovirus,<sup>33</sup> and Newcastle disease virus.<sup>13</sup> Hence, this further supports the body of evidence that the therapeutic effectiveness of oncolytic viruses is in large part due to the ICD they induce and the subsequent potent antitumor immunity this triggers.

In summary, this study shows, for the first time, the susceptibility of bladder cancer cells to CVA21 and the ability to enhance this oncolysis by modulating the expression of the viral receptor ICAM-1 by Mitomycin-C treatment. Furthermore, the utility of CVA21 as a potent immunotherapeutic agent was demonstrated by its potential to elicit several ICD-related DAMPs. The findings from this study have provided the rationale for a phase 1 clinical trial CANON (CAVATAK in non-muscle invasive bladder cancer; <https://clinicaltrials.gov/ct2/show/NCT02316171>).<sup>43</sup> The immunogenic potential of CVA21-induced death may be potentially enhanced by sequential or co-administration of other agents to increase virus uptake and oncolysis, as well as combination with immune checkpoint inhibitors.

## MATERIALS AND METHODS

### CVA21

The Kuykendall prototype strain of coxsackievirus A21 (CVA21) was obtained from Viralytics Limited (CAVATAK; Sydney, Australia). To generate heat-inactivated virus, 1 mL aliquots of virus

at  $7.5 \times 10^7$  PFU were incubated in a waterbath at 60°C for 2 hr. The absence of infectious virus was confirmed by titrating the heat-inactivated virus on the CVA21-sensitive cell line, SK-MEL-28.

### Cell Cultures and Treatments

Bladder-cancer-derived cell lines T24, 5637, TCCSUP, KU19-19, VM-CUB1, and RT-112 were obtained from ATCC. The 253J, VM-CUB2, and HCV29 cell lines were from Prof. Knowles (University of Leeds). All cell lines were authenticated by DDC Medical. Cell lines were checked monthly using MycoAlert PLUS Mycoplasma Detection Kit (Lonza). HCV29, 5637, KU19-19, and RT-112 cell lines were grown in RPMI 1640; the TCCSUP, VM-CUB1, and VM-CUB2 in DMEM; 253J in 1:1 DMEM:RPMI; J82 in EMEM; and T24 in McCoy's. Media was supplemented with 10% fetal bovine serum, penicillin/streptomycin, and glutamine.

### FACS Analysis

Bladder cancer cell lines were incubated with anti-CD54-PE or CD55-PE antibodies (BD Biosciences) and analyzed using the MACSQuantify software on a MACSQuant flow cytometer (Miltenyi Biotec). The cellular antibody-binding capacity of the cell lines was determined for anti-CD54 using BD Biosciences QuantiBRITE system (QuantiBRITE standard beads) as previously described.<sup>44</sup>

### Isolation of ICAM-1-Positive Bladder Cancer Cells

KU19-19 cells were labeled with anti-CD54(ICAM-1)-PE (BD Biosciences), washed in PBS, and resuspended in cold MACS buffer (PBS, 0.5% FBS, and 2 mmol EDTA). Superparamagnetic microbeads conjugated with monoclonal mouse anti-PE antibodies (Miltenyi Biotec, Germany) were added to the cell pellet and incubated at 4°C for 15 min. Cells were washed in cold MACS buffer before being positively selected on MS+ columns (Miltenyi Biotec).

### Immunofluorescence Detection of Infected Cells

Cell lines were seeded into chamber slides (Corning, USA) and left untreated or infected with CVA21 at the relevant MOI. After 24 hr in culture, cells were fixed using 4% paraformaldehyde. Fixed cells were incubated with rhodamine-labeled wheat germ agglutinin (Molecular Probes), washed, and permeabilized with 0.2% Triton X-100. After blocking with 10% normal goat serum, cells were stained with a mouse anti-enterovirus antibody (Clone 5-D8/1; Dako) and stained for a further 30 min with goat-anti-mouse IgG2a Alexa 488. Nuclei were stained with TO-PRO-3 (Molecular Probes). Slides were mounted with Vectashield (Vector Laboratories) and examined on a Carl Zeiss LSM 510 confocal microscope.

### Cell Viability and Cell Death Assays

Cells were infected with CVA21 MOIs at IC<sub>50</sub>, which for T24 was 11.4, 1.0 for TCCSUP, and 1.8 for 5637. Cell viability was determined 72 hr post-infection by MTS assay (Promega), and the IC<sub>50</sub> value was calculated using CalcuSyn software (Biosoft, UK).

Apoptotic cell death was determined with the annexin V-PE kit (BD Biosciences). FACS analysis was performed as above.

Caspase Glo 3/7 assay (Promega) was used to evaluate caspase 3 and 7 activity post-CVA21 infection. T24, TCCSUP, and 5637 cells were plated in 96-well plates and incubated overnight. Cells were treated with 0.5  $\mu\text{g}/\text{mL}$  Mitomycin-C and CVA21 as above. At 24, 48, and 72 hr post-treatment, Caspase Glo reagent was used as per manufacturer instructions and luminescence measured using a Varioskan Flash (Thermo Scientific) plate reader.

To confirm the death pathways involved, the pan-caspase inhibitor zVAD and the inhibitor of necroptosis, Necrostatin-1 (Sigma-Aldrich), were used. Necrostatin-1 (30  $\mu\text{M}$ ) was added 45 min prior to Mitomycin-C and/or virus addition, whereas the zVAD (20 mM) was added after Mitomycin-C and/or virus treatment. Cell viability was measured using MTS assay (Promega).

In addition, whole-cell lysates were prepared, followed by immunoblotting with anti-human PARP (no. 9542; Cell Signaling Technology, USA), anti-RIP1 (BD Biosciences), and anti-RIP-3 (Abcam) antibodies.

#### **Viral Proliferation Assays**

Viral proliferation assays were performed to assess ICAM-1-induced upregulation by Mitomycin-C on viral replication. Cells were grown in 6-well plates and treated with/without 0.5  $\mu\text{g}/\text{mL}$  Mitomycin-C for 1 hr before infecting with CVA21 at the relevant MOI for each line. Cells were exposed to CVA21 for 5 hr before washing and media replenishment. Supernatants were harvested 24, 48, and 72 hr post-infection and dilutions made from  $10^{-1}$  to  $10^{-14}$ . To determine the virus production, replication assays were performed using SK-MEL-28 cells. The CVA21 virus titer (TCID<sub>50</sub>/mL) was calculated using Spearman and Karber algorithm.

#### **ICD Determinant Analysis**

FACS analysis was used to determine expression of ICD determinants on the surfaces of treated cells. Cell lines untreated, treated with Mitomycin-C (0.5  $\mu\text{g}/\text{mL}$ ) for 1 hr, or exposed to CVA21 for 24–72 hr with or without prior Mitomycin-C treatment were harvested and incubated with anti-HSP70, anti-calreticulin, and an isotype control (Abcam). Additional stains included MHCII (BioLegend), CD80 (eBioscience), FAS (Abcam), and PD-L1 (eBioscience). Relevant secondary Alexa-488-labeled antibodies were subsequently applied (Molecular Probes).

Released HMGB1 was measured in the conditioned media of cell lines by ELISA (IBL International, Hamburg, Germany) and extracellular ATP by ATP determination kit (Molecular Probes).

#### **Vaccination Assay for the Evaluation of ICD *In Vivo***

*In vivo* procedures were approved by the UK Home Office and by AWERB of the University of Surrey. MB49 cells transfected with human ICAM-1 were treated with or without CVA21 (IC<sub>50</sub> 6.25) for 24 hr, washed, and lysates prepared. Lysates, along with HANKS media as a control, were injected subcutaneously into one flank of immunocompetent syngeneic female C57BL/6 JOLA<sup>Hsd</sup> mice

(42–49 days; Envigo). One week later, mice were re-challenged with live 1e6 MB49 cells subcutaneously into the contralateral flank.

Immunodepletion studies were conducted with mAbs anti-CD4 (GK1.5), anti-CD8 $\alpha$  (clone 2.43), anti-NK1.1 (clone PK136), and mouse IgG2a (clone C1.18.4) and rat IgG2b (clone LTF-2) isotype controls (Bio X Cell). Purified mAbs (100  $\mu\text{g}$ ) were injected intraperitoneally twice weekly starting one day before re-challenge with live 1e6 MB49 cells. The efficiency of depletion of lymphocyte subsets was measured by flow cytometry.

#### **Bladder Tumor Precision-Cut Slice Preparation and Treatment**

Tissue was obtained from consenting patients during a transurethral bladder tumor removal at the Royal Surrey County Hospital, Guildford, UK and transported to the laboratory for slicing within 1 hr. Ethics approval was given by London-Brent Research Ethics Committee study no. 12/LO/1661. Tumor tissue of small volume was embedded in 4% agarose. 300- $\mu\text{m}$  slices were prepared using the vibrating blade microtome (Leica VT1200S). Bladder tumor slices were subsequently cultured in DMEM supplemented as above. Slices were either left untreated, treated with Mitomycin-C (0.5  $\mu\text{g}/\text{mL}$ ) for 1 hr before removing the drug, or exposed to CVA21 ( $5 \times 10^6$ ) with or without prior treatment with Mitomycin-C. Cultivation was performed at 37°C and 5% CO<sub>2</sub> for 48 hr. Slices were harvested and fixed in 10% neutral-buffered formalin (Sigma Aldrich) before embedding in paraffin.

#### **Immunohistochemistry**

4- $\mu\text{m}$  paraffin sections were stained with H&E. Immunohistochemistry (IHC) staining was carried out to detect apoptosis using the TumorTACS *In Situ* Apoptosis Detection kit (Trevigen). DNA fragmentation in the tumor tissues was visualized using 3,3'-diaminobenzidine (DAB) chromogen and counterstained with 1% Methyl Green. Sections were then dehydrated and mounted.

To detect viral protein within tumor slices, 4- $\mu\text{m}$  paraffin sections were dewaxed and rehydrated before being subjected to heat-mediated antigen retrieval in a microwave using citrate buffer (10 mM; pH 6.0). Sections were incubated with an anti-enterovirus antibody (clone 5-D8/1; Dako) followed by a goat anti-mouse IgG2a-Alexa 488 and TO-PRO-3 (Molecular Probes) before mounting using Vectashield (Vector Labs). Replacement of the primary antibody by PBS/BSA 1% was used as a negative control. Results were analyzed by confocal microscopy using a LSM 510 Carl Zeiss confocal microscope.

#### **Statistical Analysis**

The GraphPad Prism software package was used to construct graphs and for statistical calculations. Each experiment was performed twice. Two-way ANOVA with Bonferroni correction was used in all *in vitro* bladder cancer cell line experiments comparing different treatment groups (untreated, Mitomycin C, CVA21, and the combination). Data comparing multiple animal groups in *in vivo* studies were also analyzed by two-way ANOVA. The one-way ANOVA with

Bonferroni correction was performed for analysis of IFN $\beta$  ELISA results. Results are shown as ( $\pm$ ) SE bars obtained from the means of each group. The following symbols were used in diagrams/figures to denote levels of significance: \* $p < 0.05$ ; \*\* $p < 0.01$ ; \*\*\* $p < 0.001$ ; and \*\*\*\* $p < 0.0001$ .

## SUPPLEMENTAL INFORMATION

Supplemental Information includes four figures and can be found with this article online at <https://doi.org/10.1016/j.omto.2018.02.001>.

## AUTHOR CONTRIBUTIONS

N.E.A., M.A., and M.D. conducted most of the experiments. N.E.A. wrote the manuscript. G.R.S. carried out the animal work. C.M.-L. carried out statistical analysis. D.M. and R.B. helped with the viral assays. D.S. and G.A. provided virus and advice on viral assays. M.K. provided cell lines. K.H. and R.V. provided intellectual input and critically read the manuscript. A.M. helped with the immunological assays. H.P. provided advice on bladder cancer and use of oncolytic viruses in the bladder.

## CONFLICTS OF INTEREST

All authors declare no conflicts of interest.

## ACKNOWLEDGMENTS

The authors acknowledge the following sources of funding: the Topic of Cancer charity and Prostate Cancer UK charity (to N.E.A.), the Prostate Project charity (to M.A. and M.D.), a DIPROMON grant (to G.R.S.), the University of Surrey (to C.M.-L., D.M., and H.P.), Viralytics (to D.S. and G.A.), the Institute of Cancer Research (to K.H. and A.M.); the Mayo Clinic (to R.V.), and NHS (to H.P.).

## REFERENCES

- Cancer Research UK (2016). Bladder cancer statistics. <http://www.cancerresearchuk.org/health-professional/cancer-statistics/statistics-by-cancer-type/bladder-cancer>.
- Aldousari, S., and Kassouf, W. (2010). Update on the management of non-muscle invasive bladder cancer. *Can. Urol. Assoc. J.* 4, 56–64.
- Fuge, O., Vasdev, N., Allchorne, P., and Green, J.S.A. (2015). Immunotherapy for bladder cancer. *Res. Rep. Urol.* 7, 65–79.
- Sanofi Pasteur (2016). Sanofi Pasteur statement on discontinuation of BCG. <http://www.sanofipasteur.ca/node/50701>.
- Davies, B. (2016). Sanofi shuts down bladder cancer drug production: inevitable drug shortage to harm patients. <https://www.forbes.com/sites/benjamindavies/2016/11/17/sanofi-shuts-down-bladder-cancer-drug-production-inevitable-drug-shortage-to-harm-patients/#27d4a3abc132>.
- Russell, S.J., Peng, K.W., and Bell, J.C. (2012). Oncolytic virotherapy. *Nat. Biotechnol.* 30, 658–670.
- Patel, M.R., and Kratzke, R.A. (2013). Oncolytic virus therapy for cancer: the first wave of translational clinical trials. *Transl. Res.* 161, 355–364.
- Tong, A.W., Senzer, N., Cerullo, V., Templeton, N.S., Hemminki, A., and Nemunaitis, J. (2012). Oncolytic viruses for induction of anti-tumor immunity. *Curr. Pharm. Biotechnol.* 13, 1750–1760.
- Steele, L., Errington, F., Prestwich, R., Ilett, E., Harrington, K., Pandha, H., Coffey, M., Selby, P., Vile, R., and Melcher, A. (2011). Pro-inflammatory cytokine/chemokine production by reovirus treated melanoma cells is PKR/NF- $\kappa$ B mediated and supports innate and adaptive anti-tumour immune priming. *Mol. Cancer* 10, 20.
- Benencia, F., Courrèges, M.C., Conejo-García, J.R., Mohamed-Hadley, A., Zhang, L., Buckanovich, R.J., Carroll, R., Fraser, N., and Coukos, G. (2005). HSV oncolytic ther-

apy upregulates interferon-inducible chemokines and recruits immune effector cells in ovarian cancer. *Mol. Ther.* 12, 789–802.

- Kroemer, G., Galluzzi, L., Kepp, O., and Zitvogel, L. (2013). Immunogenic cell death in cancer therapy. *Annu. Rev. Immunol.* 31, 51–72.
- Angelova, A.L., Grekova, S.P., Heller, A., Kuhlmann, O., Soyka, E., Giese, T., Arahamian, M., Bour, G., Ruffer, S., Cziepluch, C., et al. (2014). Complementary induction of immunogenic cell death by oncolytic parvovirus H-1PV and gemcitabine in pancreatic cancer. *J. Virol.* 88, 5263–5276.
- Koks, C.A., Garg, A.D., Ehrhardt, M., Riva, M., Vandenberk, L., Boon, L., De Vleeschouwer, S., Agostinis, P., Graf, N., and Van Gool, S.W. (2015). Newcastle disease virotherapy induces long-term survival and tumor-specific immune memory in orthotopic glioma through the induction of immunogenic cell death. *Int. J. Cancer* 136, E313–E325.
- Guo, Z.S., Liu, Z., and Bartlett, D.L. (2014). Oncolytic immunotherapy: dying the right way is a key to eliciting potent antitumor immunity. *Front. Oncol.* 4, 74.
- Shafren, D.R., Au, G.G., Nguyen, T., Newcombe, N.G., Haley, E.S., Beagley, L., Johansson, E.S., Hersey, P., and Barry, R.D. (2004). Systemic therapy of malignant human melanoma tumors by a common cold-producing enterovirus, coxsackievirus a21. *Clin. Cancer Res.* 10, 53–60.
- Au, G.G., Lindberg, A.M., Barry, R.D., and Shafren, D.R. (2005). Oncolysis of vascular malignant human melanoma tumors by Coxsackievirus A21. *Int. J. Oncol.* 26, 1471–1476.
- Berry, L.J., Au, G.G., Barry, R.D., and Shafren, D.R. (2008). Potent oncolytic activity of human enteroviruses against human prostate cancer. *Prostate* 68, 577–587.
- Skelding, K.A., Barry, R.D., and Shafren, D.R. (2009). Systemic targeting of metastatic human breast tumor xenografts by Coxsackievirus A21. *Breast Cancer Res. Treat.* 113, 21–30.
- Au, G.G., Lincz, L.F., Enno, A., and Shafren, D.R. (2007). Oncolytic coxsackievirus A21 as a novel therapy for multiple myeloma. *Br. J. Haematol.* 137, 133–141.
- Andtbacka, R., Curti, B., Hallmeyer, S., and Shafren, D.R. (2015). Abstract CT214: Phase II CALM study: Changes in the tumor microenvironment induced by the immunotherapeutic agent coxsackievirus A21 delivered intratumorally in patients with advanced melanoma. *Cancer Res.* 75, CT214.
- Liou, G.Y., Döppler, H., Necela, B., Edenfield, B., Zhang, L., Dawson, D.W., and Storz, P. (2015). Mutant KRAS-induced expression of ICAM-1 in pancreatic acinar cells causes attraction of macrophages to expedite the formation of precancerous lesions. *Cancer Discov.* 5, 52–63.
- Bamford, S., Dawson, E., Forbes, S., Clements, J., Pettett, R., Dogan, A., Flanagan, A., Teague, J., Futreal, P.A., Stratton, M.R., and Wooster, R. (2004). The COSMIC (Catalogue of Somatic Mutations in Cancer) database and website. *Br. J. Cancer* 91, 355–358.
- Kepp, O., Senovilla, L., Vitale, I., Vacchelli, E., Adjemian, S., Agostinis, P., Apetoh, L., Aranda, F., Barnaba, V., Bloy, N., et al. (2014). Consensus guidelines for the detection of immunogenic cell death. *Oncoimmunology* 3, e955691.
- Delwar, Z., Zhang, K., Rennie, P.S., and Jia, W. (2016). Oncolytic virotherapy for urological cancers. *Nat. Rev. Urol.* 13, 334–352.
- Simpson, G.R., Horvath, A., Anells, N.E., Pencavel, T., Metcalf, S., Seth, R., Peschard, P., Price, T., Coffin, R.S., Mostafid, H., et al. (2012). Combination of a fusogenic glycoprotein, pro-drug activation and oncolytic HSV as an intravesical therapy for superficial bladder cancer. *Br. J. Cancer* 106, 496–507.
- Hanel, E.G., Xiao, Z., Wong, K.K., Lee, P.W., Britten, R.A., and Moore, R.B. (2004). A novel intravesical therapy for superficial bladder cancer in an orthotopic model: oncolytic reovirus therapy. *J. Urol.* 172, 2018–2022.
- Potts, K.G., Irwin, C.R., Favis, N.A., Pink, D.B., Vincent, K.M., Lewis, J.D., Moore, R.B., Hitt, M.M., and Evans, D.H. (2017). Deletion of F4L (ribonucleotide reductase) in vaccinia virus produces a selective oncolytic virus and promotes anti-tumor immunity with superior safety in bladder cancer models. *EMBO Mol. Med.* 9, 638–654.
- Burke, J.M., Lamm, D.L., Meng, M.V., Nemunaitis, J.J., Stephenson, J.J., Arseneau, J.C., Aimi, J., Lerner, S., Yeung, A.W., Kazarian, T., et al. (2012). A first in human phase I study of CG0070, a GM-CSF expressing oncolytic adenovirus, for the treatment of nonmuscle invasive bladder cancer. *J. Urol.* 188, 2391–2397.

29. Cold Genesys (2017). Safety and efficacy of CG0070 oncolytic virus regimen for high grade NMIBC after BCG failure (BOND2). <https://clinicaltrials.gov/ct2/show/NCT02365818>.
30. Farina, M.S., Lundgren, K.T., and Bellmunt, J. (2017). Immunotherapy in urothelial cancer: recent results and future perspectives. *Drugs* 77, 1077–1089.
31. Diaz, R.M., Galivo, F., Kottke, T., Wongthida, P., Qiao, J., Thompson, J., Valdes, M., Barber, G., and Vile, R.G. (2007). Oncolytic immunovirotherapy for melanoma using vesicular stomatitis virus. *Cancer Res.* 67, 2840–2848.
32. Workenhe, S.T., Simmons, G., Pol, J.G., Lichty, B.D., Halford, W.P., and Mossman, K.L. (2014). Immunogenic HSV-mediated oncolysis shapes the antitumor immune response and contributes to therapeutic efficacy. *Mol. Ther.* 22, 123–131.
33. Diaconu, I., Cerullo, V., Hirvonen, M.L., Escutenaire, S., Ugolini, M., Pesonen, S.K., Bramante, S., Parviainen, S., Kanerva, A., Loskog, A.S., et al. (2012). Immune response is an important aspect of the antitumor effect produced by a CD40L-encoding oncolytic adenovirus. *Cancer Res.* 72, 2327–2338.
34. Prestwich, R.J., Errington, F., Ilett, E.J., Morgan, R.S., Scott, K.J., Kottke, T., Thompson, J., Morrison, E.E., Harrington, K.J., Pandha, H.S., et al. (2008). Tumor infection by oncolytic reovirus primes adaptive antitumor immunity. *Clin. Cancer Res.* 14, 7358–7366.
35. Zhang, G., Chen, F., Cao, Y., Johnson, B., and See, W.A. (2013). HMGB1 release by urothelial carcinoma cells is required for the in vivo antitumor response to Bacillus Calmette-Guérin. *J. Urol.* 189, 1541–1546.
36. Zhang, G., Chen, F., Cao, Y., Amos, J.V., Shah, G., and See, W.A. (2013). HMGB1 release by urothelial carcinoma cells in response to Bacillus Calmette-Guérin functions as a paracrine factor to potentiate the direct cellular effects of Bacillus Calmette-Guérin. *J. Urol.* 190, 1076–1082.
37. Rajani, K., Parrish, C., Kottke, T., Thompson, J., Zaidi, S., Ilett, L., Shim, K.G., Diaz, R.M., Pandha, H., Harrington, K., et al. (2016). Combination therapy with reovirus and anti-PD-1 blockade controls tumor growth through innate and adaptive immune responses. *Mol. Ther.* 24, 166–174.
38. Kennedy, R., and Celis, E. (2008). Multiple roles for CD4+ T cells in anti-tumor immune responses. *Immunol. Rev.* 222, 129–144.
39. Corthay, A., Skovseth, D.K., Lundin, K.U., Røsjø, E., Omholt, H., Hofgaard, P.O., Haraldsen, G., and Bogen, B. (2005). Primary antitumor immune response mediated by CD4+ T cells. *Immunity* 22, 371–383.
40. Mumberg, D., Monach, P.A., Wanderling, S., Philip, M., Toledano, A.Y., Schreiber, R.D., and Schreiber, H. (1999). CD4(+) T cells eliminate MHC class II-negative cancer cells in vivo by indirect effects of IFN-gamma. *Proc. Natl. Acad. Sci. USA* 96, 8633–8638.
41. Perez-Diez, A., Joncker, N.T., Choi, K., Chan, W.F., Anderson, C.C., Lantz, O., and Matzinger, P. (2007). CD4 cells can be more efficient at tumor rejection than CD8 cells. *Blood* 109, 5346–5354.
42. Miyamoto, S., Inoue, H., Nakamura, T., Yamada, M., Sakamoto, C., Urata, Y., Okazaki, T., Marumoto, T., Takahashi, A., Takayama, K., et al. (2012). Coxsackievirus B3 is an oncolytic virus with immunostimulatory properties that is active against lung adenocarcinoma. *Cancer Res.* 72, 2609–2621.
43. Vivalyics (2017). Safety and clinical activity of CAVATAK™ alone or with low dose Mitomycin C in non-muscle invasive bladder cancer (CANON). <https://clinicaltrials.gov/ct2/show/NCT02316171>.
44. Pannu, K.K., Joe, E.T., and Iyer, S.B. (2001). Performance evaluation of QuantiBRITE phycoerythrin beads. *Cytometry* 45, 250–258.

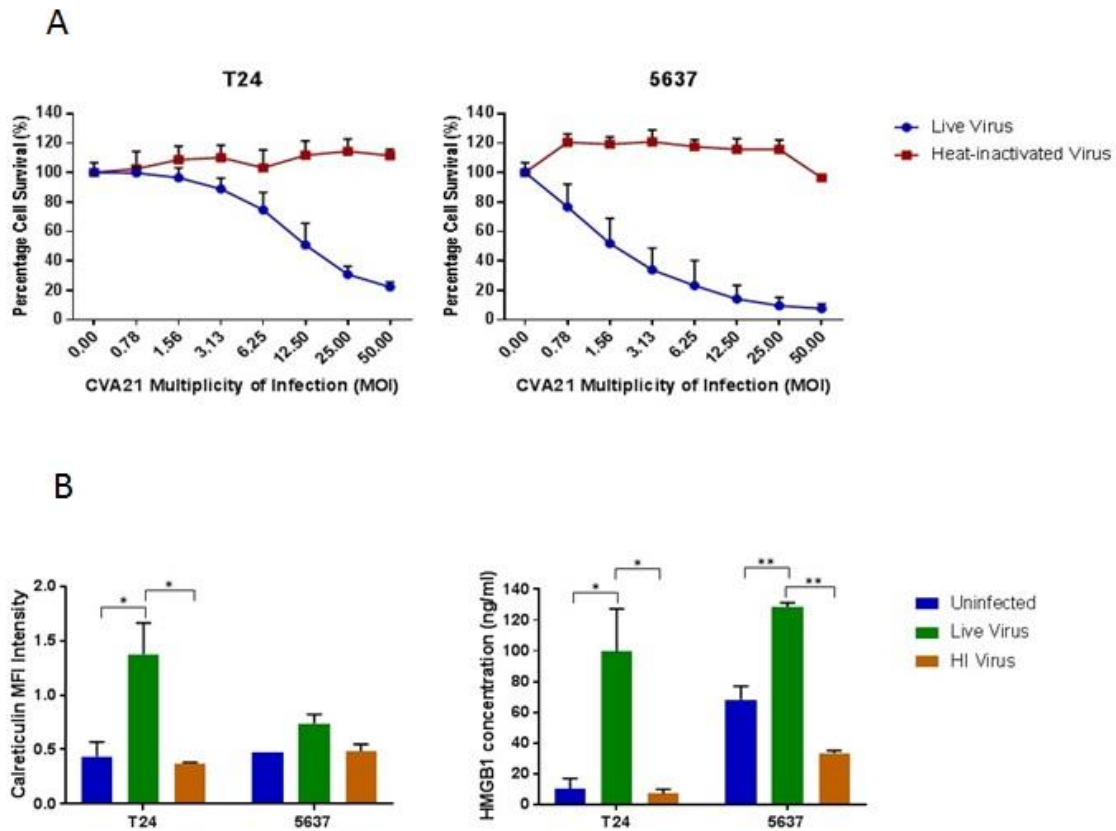
**OMTO, Volume 9**

## **Supplemental Information**

### **Oncolytic Immunotherapy for Bladder Cancer**

#### **Using Coxsackie A21 Virus**

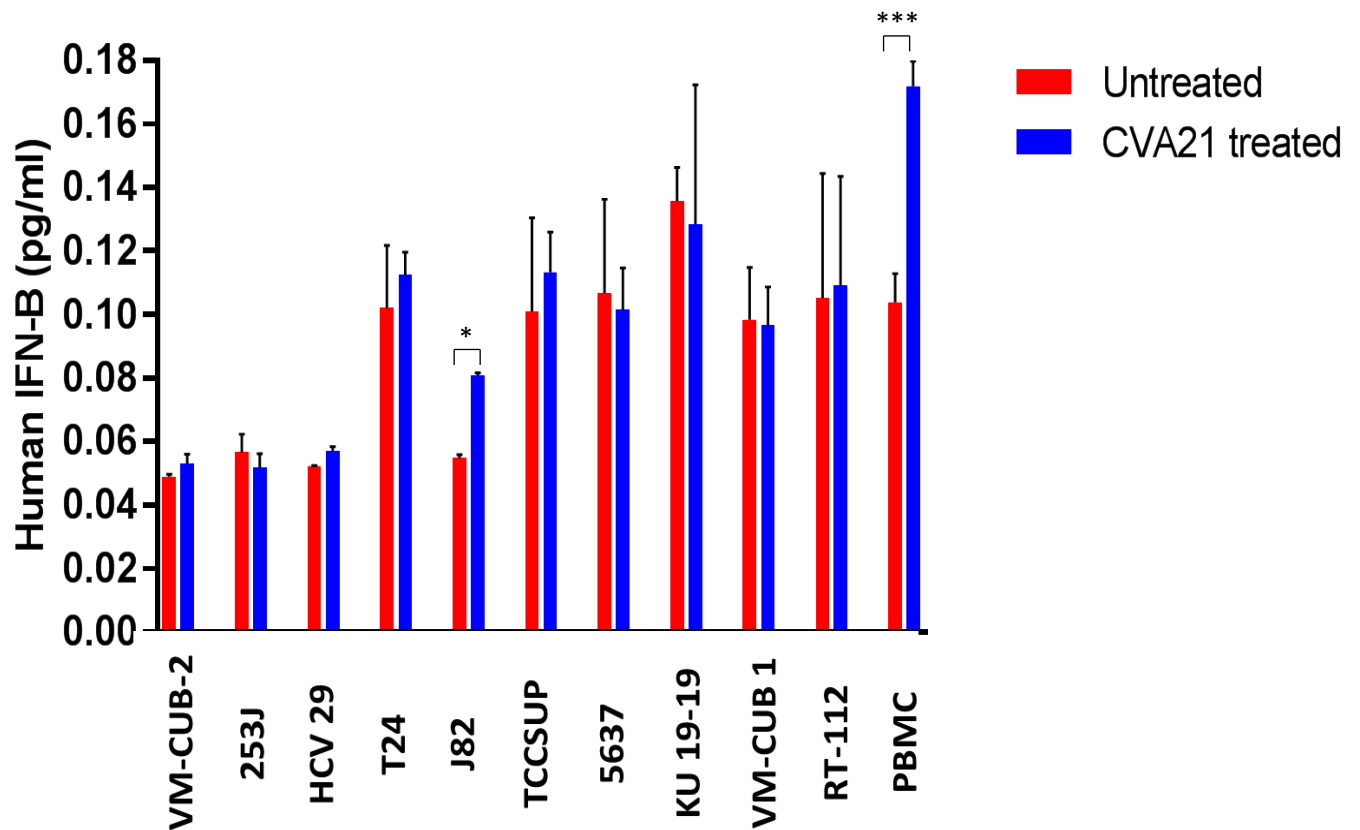
**Nicola E. Annels, Mehreen Arif, Guy R. Simpson, Mick Denyer, Carla Moller-Levet, David Mansfield, Rachel Butler, Darren Shafren, Gough Au, Margaret Knowles, Kevin Harrington, Richard Vile, Alan Melcher, and Hardev Pandha**



**Sup Fig 1. Heat-inactivated CVA21 does not affect cell viability or induce immunogenic cell death**

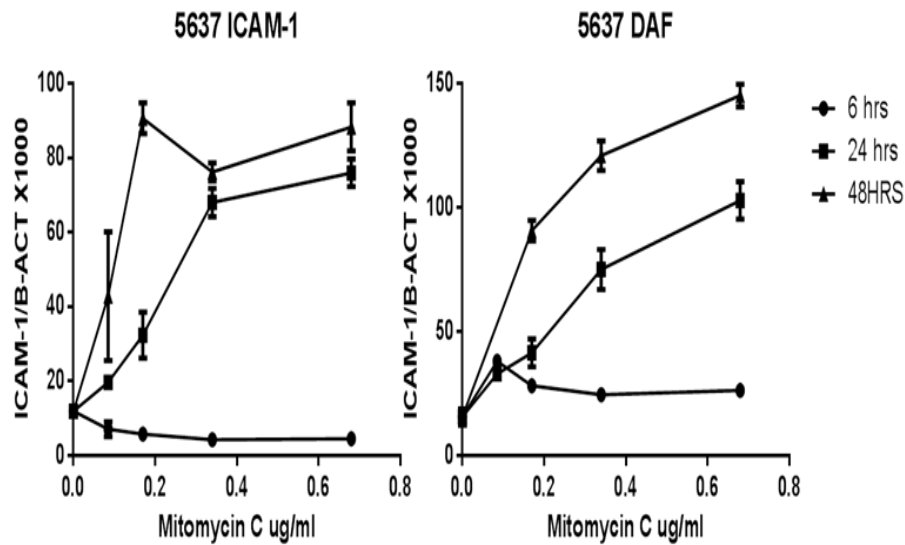
(A) Monolayer cultures of the human bladder cancer cells T24 and 5637 were challenged with increasing multiplicities of live and heat-inactivated CVA21 and assessed for cell survival at 72h post-infection, with live cells being quantified by MTS assay.

(B) The bladder cancer cell lines, T24 and 5637 were either left untreated or treated with live CVA21 or heat-inactivated CVA21. Cells and supernatants were harvested at 72h post treatment. Cell surface calreticulin (CRT) exposure was determined by FACS analysis of the cells whilst HMGB1 accumulation was determined by ELISA analysis of supernatants. Graphs represent pooled data from two independent experiments and the statistical significance of the treatment group comparisons was analysed using one-way ANOVA \* $P < 0.05$ , \*\* $P < 0.01$ , \*\*\* $P < 0.001$ , \*\*\*\* $P < 0.0001$ .



**Sup Fig 2. Interferon Beta anti-viral response was absent in all bladder cancer cell-lines except J82.**

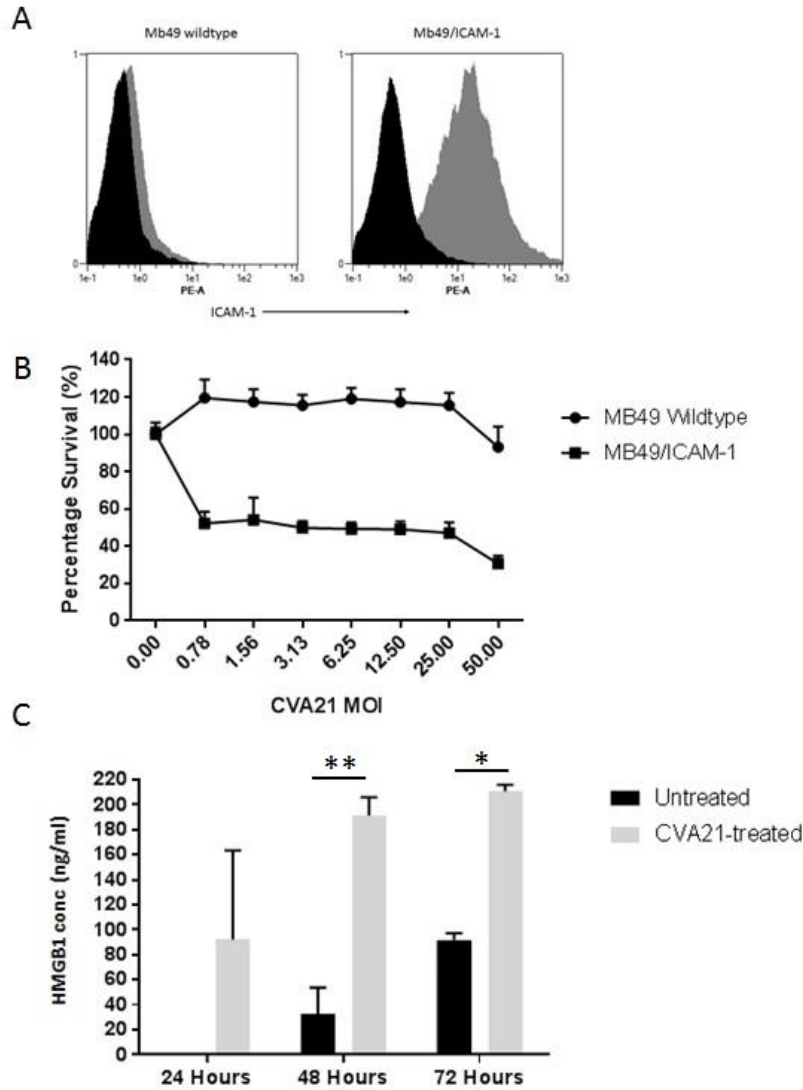
All bladder cancer cell-lines were treated with CVA21 for 24 hours and supernatant was harvested. The expression of the IFN  $\beta$  antiviral cytokine was determined by sandwich ELISA. All cell-lines displayed a lack of IFN  $\beta$  secretion after CVA21 treatment except J82 which showed a significant increase in IFN  $\beta$  post CVA21 treatment. PBMC was used as a positive control and showed a significant increase in IFN  $\beta$  production. Graphs represent pooled data from two independent experiments and one-way Anova statistical analysis was performed  $*P < 0.05$ ,  $**P < 0.01$ ,  $***P < 0.001$ ,  $****P < 0.0001$ .



**Sup Fig 3. Increased expression of ICAM-1 on bladder cancer cell lines in response to increasing doses of Mitomycin C**

The 5637 cell line was treated for 6, 24 and 48hrs with doubling dilutions of Mitomycin C up to 0.8 $\mu$ g/ml and RNA extracted. The effect of this treatment on viral receptor gene expression, ICAM-1 (A) and DAF (B) was determined by QPCR and expressed as a ratio to the amount of expression of the housekeeping gene,  $\beta$ -actin.





**Sup Fig 4. MB49 cells transfected with hICAM-1 are susceptible to the virus and display induction of the ICD determinant HMGB1**

(A) Expression of ICAM-1 on the MB49 wildtype and ICAM-1 transfected cell line (MB49/ICAM-1). Cells were incubated with either the relevant PE-conjugated isotype control antibody (black histogram), or anti-ICAM-1 monoclonal antibody (grey histogram) (B) Transfection of MB49 cells with human ICAM1 resulted in the cell line becoming susceptible to CVA21 infection compared to the wildtype MB49 as quantified by MTS assay. (C) Selective induction of HMGB1 by CVA21-treated MB49 cells determined by ELISA analysis of supernatants harvested at 24, 48 and 72h post-infection. Data represents averaged results from two independent experiments and two-way ANOVA statistical analysis was performed. \* $P < 0.05$ , \*\* $P < 0.01$ , \*\*\* $P < 0.001$ , \*\*\*\* $P < 0.0001$ .